Preprints (www.preprints.org) | NOT PEER-REVIEWED | Posted: 29 January 2020 doi:10.20944/preprints202001.0352.v1

Peer-reviewed version available at *Energies* **2020**, *13*, 1233; doi:10.3390/en13051233

Article

Flow Allocation in Meshed AC-DC Electricity Grids

Fabian Hofmann [1,†,‡], Markus Schlott [1,‡], Alexander Kies [1,*] and Horst Stöcker [1,*]

[1] Frankfurt Institute for Advanced Studies (FIAS)

* Correspondence: hofmann@fias.uni-frankfurt.de

† This paper is an extended version of our paper published in Sdewes 2019.

Abstract: In power systems, flow allocation (FA) methods allow to allocate usage and costs of the transmission grid to each single market participant. Based on predefined assumptions, the power flow is split into isolated generator specific or producer specific sub-flows. Two prominent FA methods, Marginal Participation (MP) and Equivalent Bilateral Exchanges (EBE), build upon the linearized power flow and thus on the Power Transfer Distribution Factors (PTDF). Despite their intuitive and computationally efficient concept, they are restricted to networks with *passive* transmission elements only. As soon as a significant number of *controllable* transmission elements, such as High-voltage direct current (HVDC) lines, operate in the system, they loose their applicability. This work reformulates the two methods in terms of Virtual Injection Patters (VIP) which allows to efficiently introduce a shift parameter q, tuning contributions of net sources and net sinks in the network. Major properties and differences of the methods are pointed out. Finally, it is shown how the MA and EBE algorithm can be applied to generic meshed AC-DC electricity grids: Introducing a *pseudo-impedance* $\tilde{\omega}$ which reflects the operational state of controllable elements, allows to extend the PTDF matrix under the assumption of knowing the current system's flow. Basic properties from graph theory are used for solving the pseudo-impedance dependent on the position in the network. This directly enables *e.g.* HVDC lines to be considered in the MP and EBE algorithm. The extended methods are applied to a low-carbon European network model (PyPSA-EUR) with a spatial resolution of N=181 and an 18% transmission expansion. The allocations of VIP and MP, show that countries with high wind potentials profit most from the transmission grid expansion. Based on the average usage of transmission system expansion a method of distributing operational and capital expenditures is proposed. Further it is shown, how injections from renewable resources strongly drive country-to-country allocations and thus cross-border electricity flows.

Keywords: Power System Analysis; Flow Allocation; Transmission Cost Allocation; European Electricity Grid

1. Introduction

The shift from conventional to renewable power sources requires high investments not only on the generation side but also on the transmission and storage side of a power system. Due to the dominant dependence on fluctuating wind and solar power potentials, energy has to be shifted in space and time. For large networks, as the European power system, both elements will play a key role. Spatial balancing, via a solid transmission grid, will allow power to cover long distances from wind farms far from load centers. In contrast, temporal balancing allows more self-sufficient areas which locally produce and store (most likely solar) power. This raises the question of who uses and profits to what extent from the transmission grid and its upcoming expansions. Flow allocation (FA) methods allow to efficiently quantify the transmission usage per market-participant by decomposing the network flow into sub-flows driven by isolated power injections. On one hand this opens the opportunity to distribute transmission costs based on the effective transmission usage of each single generator and consumer, as broadly reviewed in [1]. On the other hand it helps to understand the operational state of the system and to determine cost-extensive and cost-reducing actions, which helps to draw up incentives or cost-schemes for an efficient system transformation.

© 2020 by the author(s). Distributed under a Creative Commons CC BY license.

Preprints (www.preprints.org) | NOT PEER-REVIEWED | Posted: 29 January 2020 doi:10.20944/preprints202001.0352.v1

Peer-reviewed version available at Energies 2020, 13, 1233; doi:10.3390/en13051233

There exist multiple flow allocation methods all differently approaching the determination of isolated sub-flows. The most prominent candidates happen to be:

(a) Average Participation, also named Flow Tracing, firstly presented in [2] and used in various application cases as in [3]. It follows the principle of proportional sharing when tracing a power flow from source to sink
(b) Z-bus transmission allocation presented in [4] which is equivalent to the Power Divider method [5] and very related to the formulation in [6]. It derives the contributions of electricity current injections to the branch currents based on the full AC power flow equations.
(c) Marginal Participation (MP) presented in [7] and (d) Equivalent Bilateral Exchanges (EBE) method [8] which are based on the linearized power flow equations and extensively explained later in this paper.
(e) With-And-Without transits loss allocation presented in [9] which builds the underlying loss allocation for the Inter-Transmission System Operators Compensation (ITC) mechanism. In contrast to the other methods it does not determine source-sink relations but calculates losses within regions or countries caused by cross-border flows.

Non flow-based cost allocation includes another pallette of methods, such as a 'Aumann-Shapley' method [10] which is based on Game Theory or an exogenous approach [11] which proposes to introduce a peer-to-peer market design into the optimal power flow (OPF) calculation. Originally, the FA methods focus on determining the flow shares on branches. However the work in [12] shows that the FA can be alternatively represented through Virtual Injection Patterns (VIP), that are peer-to-peer allocations between sources and sinks. Thus, every market generator is associated to a specific set of supplied loads and, vice versa, loads are allocated to a specific set of power suppliers from which they retrieve their share. The artificial peer-to-peer transactions can then be used to *e.g* determine nodal electricity prices or the CO_2-intensity of the consumed power, as done in a recent study [13]. As all FA methods come along with strengths and weaknesses, it turns out that most of them are restricted to pure AC or pure passive DC transmission networks only. This applies to non-linear FA as well as MP and EBE, which rely on the linear Power Transfer Distribution Factors (PTDF). It makes them inappropriate for large networks, likewise the European one, which consists of multiple AC *subnetworks*, i.e. synchronous zones operating at a specific utility frequency. So far the PTDF-based allocation is not applicable over borders of these zones and only conceptional propositions have been made to tackle this issue [14]. Note that also FA on distribution network level are inappropriate for the MP and EBE algorithm, as the characteristic of high resistance-reactance ratios render the linear approximation of the power flow invalid. This restricts the scope of application for the MP and EBE algorithms considerably. However, in the following it is shown, how the two algorithms can be applied to meshed AC-DC transmission networks by incorporating controllable elements as HVDC lines into the PTDF matrix.

The paper is structured as follows: Sec. 2 recalls the MP and EBE algorithms, focusing on both VIP and flow share formulation. Sec. 3 describes the extension of the flow allocation methods for generic AC-DC networks, realized through the introduction of the so-called pseudo-reactance $\bar{\omega}$. In Sec. 4 the extended FA is performed for a highly renewable European power system and Sec. 5 summarizes and concludes the paper.

Preprints (www.preprints.org) | NOT PEER-REVIEWED | Posted: 29 January 2020 doi:10.20944/preprints202001.0352.v1

Peer-reviewed version available at Energies 2020, 13, 1233; doi:10.3390/en13051233

2. PTDF Based Flow Allocation Methods

The Marginal Participation (MP) and Equivalent Bilateral Exchanges (EBE) algorithms are both based on the linear power flow approximation. In order to recall and extent them, let the following quantities be defined throughout this work

Nodal active power	$\mathbf{p} \in \mathbb{R}^N$	PTDF matrix	$\mathbf{H} \in \mathbb{R}^{L\times N}$
Active power flow	$\underline{\mathbf{f}} \in \mathbb{R}^L$	Cycle matrix	$\mathbf{C} \in \mathbb{R}^{L\times C}$
Transmission reactance	$\underline{\mathbf{x}} \in \mathbb{R}^L$	Virtual Injection Pattern	$\tilde{\mathbf{P}} \in \mathbb{R}^{N\times N}$
Transmission resistance	$\underline{\mathbf{r}} \in \mathbb{R}^L$	Virtual Flow Pattern	$\tilde{\mathbf{F}} \in \mathbb{R}^{L\times N}$
Transmission admittance	$\underline{\mathbf{y}} \in \mathbb{C}^L$	Peer-to-Peer Allocations	$\mathbf{A} \in \mathbb{R}^{N\times N}$
Incidence matrix	$\mathbf{K} \in \mathbb{R}^{N\times L}$		

where N denotes the number of buses in the system, L the number of branches (transmission lines) and C the number of cycles in the network. Note that the equality C = L - N + 1 holds as shown by Ronellenfitsch et al. [15,16]. The linear power flow approximation assumes that all bus voltage magnitudes are equal, $\hat{v}_i = \hat{v}_j$, and the series resistances are small compared to series reactances, $r_l \ll x_l$. Further, voltage angle differences across a line are assumed to be small and no shunt admittances (at buses or series) to ground are present. These assumptions are usually appropriate for transmission systems, where high voltages and small resistances lead to a power flow which is mostly driven by active power injection $\mathbf{p}$. They allow to map the latter linearly to the active power flow $\underline{\mathbf{f}}$ through the PTDF matrix

$$\underline{\mathbf{f}} = \mathbf{H}\,\mathbf{p} \tag{1}$$

where the PTDF matrix is defined as

$$\mathbf{H} = \mathrm{diag}\left(\underline{\mathbf{y}}\right)\mathbf{K}^T\left(\mathbf{K}\,\mathrm{diag}\left(\underline{\mathbf{y}}\right)\mathbf{K}^{\mathrm{T}}\right)^{+} \tag{2}$$

with the series admittance $\underline{\mathbf{y}} = \underline{\mathbf{x}}^{-1}$ and $()^+$ denoting the generalized inverse. We recall that the PTDF matrix can be provided with a slack, that is one or more buses which 'absorb' total power imbalances of $\mathbf{p}$. In formulation (2) the slack is distributed over all nodes in the system, however it is possible to modify it by adding a column vector $\mathbf{k}$ to the PTDF matrix

$$\mathbf{H} \to \mathbf{H} + \mathbf{k} \tag{3}$$

without touching the result of the linear power flow equation (1) for a balanced injection pattern. Corresponding to equation (1), the nodal power balance is expressed by

$$\mathbf{p} = \mathbf{K}\,\underline{\mathbf{f}} \tag{4}$$

As pointed out earlier, the FA methods can be perceived from two different angles. One is looking at the impact of generators or consumers on the network flow they cause in the network respectively. The Virtual Flow Pattern (VFP) matrix $\tilde{\mathbf{F}}$ is a L $\times$ N matrix of which the nth column denotes the sub-flow induced by bus n. The other is looking at the peer-to-peer transactions given by the Virtual Injection Pattern matrix $\tilde{\mathbf{P}}$ of size N $\times$ N of which the nth column denotes the effective, balanced injection pattern of bus n. The two quantities contain the same information and are, similarly to equations (1) and (4), linked through

$$\tilde{\mathbf{F}} = \mathbf{H}\,\tilde{\mathbf{P}} \tag{5}$$

Preprints (www.preprints.org) | NOT PEER-REVIEWED | Posted: 29 January 2020 doi:10.20944/preprints202001.0352.v1

Peer-reviewed version available at Energies 2020, 13, 1233; doi:10.3390/en13051233

and

$$\tilde{\mathbf{P}} = \mathbf{K}\,\tilde{\mathbf{F}} \tag{6}$$

Further the sum of their columns equals the original flow

$$\underline{\mathbf{f}} = \tilde{\mathbf{F}}\,\mathbf{1}_N \tag{7}$$

and the original injection pattern respectively

$$\mathbf{p} = \tilde{\mathbf{P}}\,\mathbf{1}_N \tag{8}$$

where $\mathbf{1}_N$ represents a vector of ones of length N. Further let $\mathbf{A}$ denotes a $N \times N$ matrix with peer-to-peer transactions $m \rightarrow n$ given by the entry A_{mn}. For a given VIP matrix, those values are straightforwardly obtained by $\tilde{P}_{mn} - \tilde{P}_{nm}$, that is taking all power in the injection pattern of n coming from m to n and all the *negative* power in the injection pattern of n coming from m. In matrix notation this leads to

$$\mathbf{A} = \left(\tilde{\mathbf{P}} - \tilde{\mathbf{P}}^{\mathrm{T}}\right)_+ \tag{9}$$

where $()_+$ denotes to restrict to positive entries only. The latter should be taken for granted as only positive source to sink relations are considered. Thus, for non-zero values A_{mn}, bus m is always a net producer and bus n a net consumer.

Equivalent Bilateral Exchanges

The definition of the EBE algorithm refers to peer-to-peer exchanges between net producers (sources) and net consumers (sinks) in the network [8]. It assumes that a source provides all sinks in the network which are proportionally scaled down while all other sources are ignored. Correspondingly, it assumes that power flowing into a sink comes from all sources which are proportionally scaled down while all other sinks are ignored. In order to allow weighting the net producers differently from net consumers, let $0 \leq q \leq 1$ be a shift parameter which allows tuning their contributions (the lower, the stronger net consumers are taken into account). Further, let $\mathbf{p}_{+/-}$ denote injections by only sources/sinks and let $\gamma = \left(\mathbf{p}_+^{\mathrm{T}}\,\mathbf{1}_{(N)}\right)^{-1}$ denote the inverse of the total positive injected power. Therefore the VIP is given by

$$\tilde{\mathbf{P}}_{\mathrm{ebe}} = q\left(\mathbf{P}_+ + \gamma\,\mathbf{p}_-\mathbf{p}_+^{\mathrm{T}}\right) + (1-q)\left(\mathbf{P}_- - \gamma\,\mathbf{p}_+\mathbf{p}_-^{\mathrm{T}}\right) \tag{10}$$

The first term represents injection patterns of net producers only which deliver power to sinks. The second term comprises injection patterns of all net consumers. The corresponding VFP matrix $\tilde{\mathbf{F}}_{\mathrm{ebe}}$ is given by

$$\tilde{\mathbf{F}}_{\mathrm{ebe}}(q) = \mathbf{H}\,\tilde{\mathbf{P}}_{\mathrm{ebe}}(q) \tag{11}$$

If q is set to 0.5, 50% of the flow is allocated to net producers and 50% to net consumers. Inserting (10) into (11) allows to write the VFP in form of

$$\tilde{\mathbf{F}}_{\mathrm{ebe}} = \mathbf{H}\,\mathbf{P} \tag{12}$$

with a given slack of $\mathbf{k} = \gamma\,\underline{\mathbf{f}}_-$ for net producers and $\mathbf{k} = -\gamma\,\underline{\mathbf{f}}_+$ for net consumers in the PTDF matrix (see eq. (3)). It is taken as granted that the separate flow patterns induced by the market participants

Preprints (www.preprints.org) | NOT PEER-REVIEWED | Posted: 29 January 2020 doi:10.20944/preprints202001.0352.v1

Peer-reviewed version available at Energies 2020, 13, 1233; doi:10.3390/en13051233

can be of completely different nature than the original flow. Therefore the FA method may leads to *counter-flows* which are counter aligned to the network flow $\underline{\mathbf{f}}$.

Given that $\mathbf{p} = \mathbf{p}_+ + \mathbf{p}_-$, the peer-to-peer relations are straightforwardly obtained by first, reformulating (10) to

$$\tilde{\mathbf{P}}_{\text{ebe}} = \mathbf{P}_- - \gamma\, \mathbf{p}_+ \mathbf{p}_-^{\mathrm{T}} + \underbrace{q\left(|\mathbf{P}| + \gamma\, \mathbf{p}_-\, \mathbf{p}_+^{\mathrm{T}} + \gamma\, \mathbf{p}_+\, \mathbf{p}_-^{\mathrm{T}}\right)}_{\text{symmetric}} \tag{13}$$

and second, inserting the new expression into (9) ($|\cdot|$ denotes the absolute value). Note, that the symmetric term cancels out, which makes $\mathbf{A}$ independent of q, and finally boils it down to

$$\mathbf{A}_{\text{ebe}} = -\gamma\, \mathbf{p}_+\, \mathbf{p}_-^{\mathrm{T}} \tag{14}$$

which one-on-one reflects the definition of the EBE flow allocation.

Marginal Participation

The MP algorithm, in contrast to EBE, comes from a sensitivity analyzing perspective which directly defines the VFP matrix. As originally proposed, it measures each line's active power flow sensitivity against changes in the power balances of the buses. The sensitivity characteristics are then multiplied with the nodal power imbalances, which gives the sub-flows induced by the buses. As the work in [14] describes in detail, the choice of the slack $\mathbf{k}$ is used for tuning contributions of net producers and net consumers. However, aiming at introducing the shift parameter q correctly and in an generalized way, we propose straightforwardly to define the VIP matrix as

$$\tilde{\mathbf{P}}_{\text{mp}} = \tilde{\mathbf{P}}_{\text{ebe}} + s\left(\mathbf{P} + \gamma\, \mathbf{p}_-\mathbf{p}_-^{\mathrm{T}} - \gamma\, \mathbf{p}_+\mathbf{p}_+^{\mathrm{T}}\right) \tag{15}$$

where s is set to $s = \frac{1}{2} - \left|q - \frac{1}{2}\right|$. Here, we used the full VIP pattern for the EBE method and added a term which only takes effect for $0 < q < 1$. This makes $\tilde{\mathbf{P}}_{\text{mp}}$ and $\tilde{\mathbf{P}}_{\text{ebe}}$ the same for full allocation to consumers ($q = 0$) or producers ($q = 1$). The standard 50%-50% split leads to

$$\tilde{\mathbf{P}}_{\text{mp}}(q = 0.5) = \mathbf{P} - \frac{1}{2}\gamma\, |\mathbf{p}|\, \mathbf{p}^{\mathrm{T}} \tag{16}$$

which, when inserting into (5), leads to an effective slack of

$$\mathbf{k}_{\text{mp}}(q = 0.5) = \frac{1}{2}\,\gamma\,(\underline{\mathbf{f}}_- - \underline{\mathbf{f}}_+) \tag{17}$$

which reflects the standard setup of the MP algorithm as originally proposed. Overall, the newly introduced formulation given in eq. (15) generalizes the algorithm for the shift parameter q and matches the EBE method for full consumer/producer contributions. Again note that the $\tilde{\mathbf{F}}_{\text{MP}}$ may contain counter-flows which are not aligned with $\underline{\mathbf{f}}$. Especially in the realm around $q = 0.5$ this is even more likely for the MP method, as flows are also allocated from one net producer to another net producer. It shall be noted that the second term in eq. (15) is symmetric, which makes the peer-to-peer allocation again independent of the shift parameter q, which leads to

$$\mathbf{A}_{\text{mp}} = -\gamma\, \mathbf{p}_+\, \mathbf{p}_- = \mathbf{A}_{\text{ebe}} \tag{18}$$

So, it can the be concluded that the peer-to-peer relations for both EBE and MP are the same, whereas the flow allocations and virtual injections patterns differ for mixed producer-consumer contributions.

Preprints (www.preprints.org) | NOT PEER-REVIEWED | Posted: 29 January 2020 doi:10.20944/preprints202001.0352.v1

Peer-reviewed version available at Energies 2020, 13, 1233; doi:10.3390/en13051233

3. Including Controllable Elements in the PTDF Formulation

Despite representing the two methods in form of Virtual Injection Patterns, eqs. (10) and (15), the flow allocation in form of (5) is still restricted to the scope of the PTDF matrix, namely to AC-subnetworks or pure passive DC networks. Up to now, proposals for incorporating HVDC lines within the MP or EBE [14,17] are rather of conceptional nature and do not derive all mathematical details. In the following, it is shown how the PTDF matrix can be reformulated and extended by introducing a flow-dependent *pseudo-impedance* $\bar{\omega}\left(\underline{\mathbf{f}}\right)$ for controllable DC lines, which here shall represent all controllable branch elements. The resulting extended PTDF matrix then solves Equation (1) for mixed AC-DC networks.

In a network of N nodes and L lines, let there be $\mathrm{L_{AC}}$ AC lines, $\mathrm{L_{PDC}}$ passive DC lines and $\mathrm{L_{CDC}}$ controllable DC lines. As stated in [15], a graph can always be decomposed into cycles and trees. Due to different physical laws, the two cases are treated separately, in terms of a DC line being part of a cycle in the network (**Case 1**) or being part of a tree in the network (**Case 2**).

3.1. Controllable Elements in Cycles (Case 1)

Let $\mathbf{C}^{\mathrm{AC}}$ denote the cycle matrix for all pure AC line cycles and $\underline{\mathbf{f}}^{\mathrm{AC}} \in \mathbb{R}^{\mathrm{L_{AC}}}$ be the flow on all AC lines, then, according to the linear approximation, the Kirchhoff Voltage Law states that the flows in every closed cycle weighted by the reactants sum up to zero, namely

$$\mathbf{C}^{\mathrm{AC}}\,\mathrm{diag}\left(\underline{\mathbf{x}}\right)\underline{\mathbf{f}}^{\mathrm{AC}} = 0. \tag{19}$$

As a counterpart, let $\mathbf{C}^{\mathrm{PDC}}$ be the cycle matrix for *passive* DC lines and $\underline{\mathbf{f}}^{\mathrm{DC}}_{\mathrm{passive}}$ the flow on those lines. Then Ohm's law states that flows in a closed cycle weighted by underlying resistance sum up to zero

$$\mathbf{C}^{\mathrm{PDC}}\,\mathrm{diag}\left(\underline{\mathbf{r}}\right)\underline{\mathbf{f}}^{\mathrm{DC}}_{\mathrm{passive}} = 0. \tag{20}$$

In a network with pure AC subnetworks and pure passive DC subnetworks, $\underline{\mathbf{x}}$ and $\underline{\mathbf{r}}$ are not overlapping. Equation (19) and (20) can thus be combined by using $\underline{\mathbf{z}} = \begin{bmatrix}\underline{\mathbf{r}} & \underline{\mathbf{x}}\end{bmatrix}^{\mathrm{T}}$, $\underline{\mathbf{z}} \in \mathbb{R}^{L-L_{\mathrm{CDC}}}$ and collecting the flows on all passive branches in $\underline{\mathbf{f}}_{\mathrm{passive}} = \begin{bmatrix}\underline{\mathbf{f}}^{\mathrm{AC}} & \underline{\mathbf{f}}^{\mathrm{DC}}_{\mathrm{passive}}\end{bmatrix}^{\mathrm{T}}$, which leads to

$$\begin{bmatrix}\mathbf{C}^{\mathrm{AC}} \\ \mathbf{C}^{\mathrm{PDC}}\end{bmatrix}\mathrm{diag}\left(\underline{\mathbf{z}}\right)\underline{\mathbf{f}}_{\mathrm{passive}} = 0. \tag{21}$$

Note that flows on controllable DC lines are not considered in equation (21) as those are not given by physical laws and not a function of $(\mathbf{C}, \underline{\mathbf{r}}, \mathbf{p})$. In order to include controllable DC lines, let $\mathbf{C}^{\mathrm{mixed}}$ denote the cycle matrix with all cycles in which (I) controllable DC lines with nonzero flow appear and (II) no controllable DC line with zero flow. Note that (II) guarantees that topologically irrelevant cycles are excluded as controllable DC with zero flow are not affecting the total flow pattern. We introduce a *pseudo-impedance* $\bar{\omega} \in \mathbb{R}^{L_{\mathrm{CDC}}}$ for controllable DC lines, which fulfills equation

$$\mathbf{C}\,\mathrm{diag}\left(\begin{bmatrix}\underline{\mathbf{z}} \\ \bar{\omega}\end{bmatrix}\right)\underline{\mathbf{f}} = 0, \tag{22}$$

where $\mathbf{C}$ denotes all cycles in the AC/DC super grid in the form $\mathbf{C} = \begin{bmatrix}\mathbf{C}^{\mathrm{AC}} & \mathbf{C}^{\mathrm{PDC}} & \mathbf{C}^{\mathrm{mixed}}\end{bmatrix}^{\mathrm{T}}$ and $\underline{\mathbf{f}}$ the full network flow in the form $\underline{\mathbf{f}} = \begin{bmatrix}\underline{\mathbf{f}}_{\mathrm{passive}} & \underline{\mathbf{f}}_{\mathrm{control.}}\end{bmatrix}^{\mathrm{T}}$. In order to solve equation (22) for $\bar{\omega}$, we only

Preprints (www.preprints.org) | NOT PEER-REVIEWED | Posted: 29 January 2020 doi:10.20944/preprints202001.0352.v1

Peer-reviewed version available at Energies 2020, 13, 1233; doi:10.3390/en13051233

consider mixed cycles, as all other cycles are not affected by $\bar{\omega}$. We then split the mixed cycle matrix into two parts, according to $\mathbf{C}^{\text{mixed}} = \left[\mathbf{C}^{\text{mixed}}_{\text{passive}} \; \mathbf{C}^{\text{mixed}}_{\text{control.}}\right]$

$$0 = \mathbf{C}^{\text{mixed}} \operatorname{diag}\left(\begin{bmatrix}\underline{\mathbf{z}}\\ \bar{\omega}\end{bmatrix}\right) \underline{\mathbf{f}} \tag{23}$$

$$= \left[\mathbf{C}^{\text{mixed}}_{\text{passive}} \; \mathbf{C}^{\text{mixed}}_{\text{control.}}\right] \operatorname{diag}\left(\begin{bmatrix}\underline{\mathbf{z}}\\ \bar{\omega}\end{bmatrix}\right) \begin{bmatrix}\underline{\mathbf{f}}_{\text{passive}}\\ \underline{\mathbf{f}}_{\text{control.}}\end{bmatrix} \tag{24}$$

$$= \mathbf{C}^{\text{mixed}}_{\text{control.}} \operatorname{diag}\left(\bar{\omega}\right) \underline{\mathbf{f}}_{\text{control.}} + \mathbf{C}^{\text{mixed}}_{\text{passive}} \operatorname{diag}\left(\underline{\mathbf{z}}\right) \underline{\mathbf{f}}_{\text{passive}} \tag{25}$$

$$= \mathbf{C}^{\text{mixed}}_{\text{control.}} \operatorname{diag}\left(\underline{\mathbf{f}}_{\text{control.}}\right) \bar{\omega} + \mathbf{C}^{\text{mixed}}_{\text{passive}} \operatorname{diag}\left(\underline{\mathbf{z}}\right) \underline{\mathbf{f}}_{\text{passive}} \tag{26}$$

In the last step it was used that for any equally shaped vectors $\mathbf{a}$ and $\mathbf{b}$, the relation $\operatorname{diag}(\mathbf{a})\,\mathbf{b} = \operatorname{diag}(\mathbf{b})\,\mathbf{a}$ is valid. Isolating $\bar{\omega}$ in Equation (26) leads to

$$\bar{\omega} = -\left(\mathbf{C}^{\text{mixed}}_{\text{control.}} \operatorname{diag}\left(\underline{\mathbf{f}}_{\text{control.}}\right)\right)^{+} \mathbf{C}^{\text{mixed}}_{\text{passive}} \operatorname{diag}\left(\underline{\mathbf{z}}\right) \underline{\mathbf{f}}_{\text{passive}} \tag{27}$$

Figuratively, the pseudo-impedance stands for the reciprocal contribution of a DC line to the current flow $\underline{\mathbf{f}}$ within the considered cycle. It indicates the impedance a controllable DC line would have, if it were a passive AC line. Hence, the higher the flow on a DC line the lower its pseudo-impedance.
In Figure 1 we give a short example of DC lines embedded in cycles in a network with N = 4, L_{AC} = 2 and L_{CDC} = 3. The pseudo-impedance in (28) directly results from the first four quantities, namely the Incidence Matrix, flow, injection and reactance. The arrow sizes in Figure 1 are proportionally set to their flow.

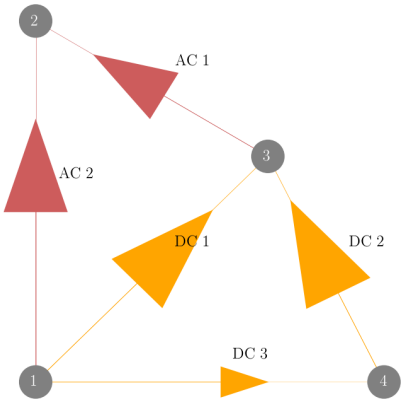

Figure 1. Example for pure cycle network with both AC and controllable DC lines (**Case 1**). When creating a PTDF matrix for such a flow pattern the pseudo-impedance values for the DC lines are given by equation (27). Relevant corresponding network quantities are given in equation (28).

Preprints (www.preprints.org) | NOT PEER-REVIEWED | Posted: 29 January 2020 doi:10.20944/preprints202001.0352.v1

Peer-reviewed version available at Energies 2020, 13, 1233; doi:10.3390/en13051233

$$\mathbf{K} = \begin{bmatrix} 0 & 1 & 1 & 0 & 1 \\ 1 & -1 & 0 & 0 & 0 \\ -1 & 0 & -1 & 1 & 0 \\ 0 & 0 & 0 & -1 & -1 \end{bmatrix}, \quad \mathbf{p} = \begin{bmatrix} 10 \\ -7 \\ -7 \\ 4 \end{bmatrix}, \quad \begin{bmatrix} \underline{\mathbf{f}}^{\mathrm{AC}} \\ \underline{\mathbf{f}}^{\mathrm{DC}} \end{bmatrix} = \begin{bmatrix} -3 \\ 4 \\ 5 \\ -5 \\ 1 \end{bmatrix}, \quad \underline{\mathbf{x}} = \begin{bmatrix} 0.5 \\ 0.5 \end{bmatrix}, \quad \begin{bmatrix} \underline{\mathbf{z}} \\ \bar{\omega} \end{bmatrix} = \begin{bmatrix} 2 \\ 2 \\ 10 \\ 10 \\ 52 \end{bmatrix} \tag{28}$$

3.2. Controllable Elements in Tree Networks (Case 2)

If the controllable DC lines are not embedded in cycles, one can consider them as topologically being a part of a tree network. For such a tree network with $\mathrm{L} < \mathrm{N}$, the Incidence matrix is non-singular. Thus, equation (1) is straightforwardly derived from Equation (4) as $\mathbf{H} = \mathbf{K}^{+}$ is well-defined. Further, extracting values for the pseudo-impedance becomes trivial as

$$\operatorname{diag}\left(\underline{\mathbf{y}}\right) \mathbf{K}^{T} \left(\mathbf{K} \operatorname{diag}\left(\underline{\mathbf{y}}\right) \mathbf{K}^{\mathrm{T}}\right)^{+} = \mathbf{K}^{+} \tag{29}$$

is solved by $\underline{\mathbf{y}}^{\mathrm{DC}}_{\text{control.}} = 1$ where $\underline{\mathbf{y}} = \left[\underline{\mathbf{y}}_{\text{passive}}\ \underline{\mathbf{y}}_{\text{control.}}\right]^{\mathrm{T}}$ and thus $\bar{\omega} = 1$.
Again, we show a small example for a tree network of N = 6, $\mathrm{L_{CDC}} = 4$ and $\mathrm{L_{AC}} = 1$ with given flows and injections (30) and topology shown in Figure 2.

$$\mathbf{K} = \begin{bmatrix} 0 & 1 & 0 & 0 & 0 \\ 1 & 0 & 0 & 0 & 0 \\ -1 & -1 & 1 & 0 & 0 \\ 0 & 0 & -1 & 1 & 1 \\ 0 & 0 & 0 & -1 & 0 \\ 0 & 0 & 0 & 0 & -1 \end{bmatrix}, \quad \mathbf{p} = \begin{bmatrix} 8 \\ -7 \\ 0 \\ 0 \\ -7 \\ 6 \end{bmatrix}, \quad \begin{bmatrix} \underline{\mathbf{f}}^{\mathrm{AC}} \\ \underline{\mathbf{f}}^{\mathrm{DC}} \end{bmatrix} = \begin{bmatrix} -7 \\ 8 \\ 1 \\ 7 \\ -6 \end{bmatrix}, \quad \underline{\mathbf{x}} = \begin{bmatrix} 0.5 \end{bmatrix}, \quad \begin{bmatrix} \underline{\mathbf{z}} \\ \bar{\omega} \end{bmatrix} = \begin{bmatrix} 2 \\ 1 \\ 1 \\ 1 \\ 1 \end{bmatrix} \tag{30}$$

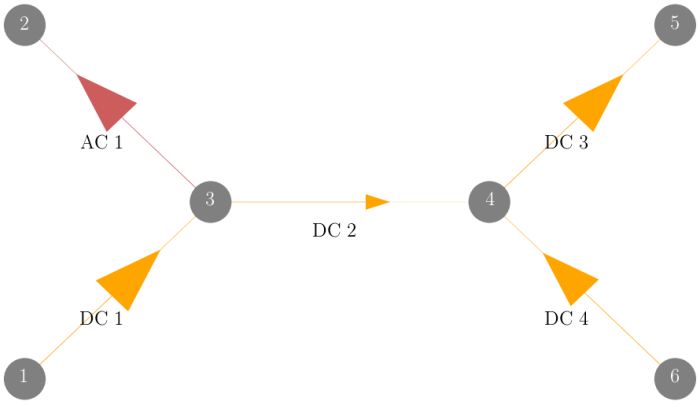

Figure 2. Example of a pure tree network with both AC and DC lines (**Case 2**). In the PTDF matrix the pseudo-impedance values for the DC lines are trivially 1 for the given flow pattern.

The extended impedance in the form of $\left[\underline{\mathbf{z}}\ \bar{\omega}\right]^{\mathrm{T}}$ can now be inserted in eq. (3) by replacing $\underline{\mathbf{y}}$ by its inverse. The resulting PTDF matrix now solves eq. (1) for a meshed AC-DC network.

Preprints (www.preprints.org) | NOT PEER-REVIEWED | Posted: 29 January 2020 doi:10.20944/preprints202001.0352.v1

Peer-reviewed version available at Energies 2020, 13, 1233; doi:10.3390/en13051233

4. Flow Allocation across European Synchronous Zones

In the following the formalism presented in sections 2 and 3 is applied to a highly renewable European network model in order to extract general sink-source relations and transmission flow behavior. We show how cross-border flows are mainly driven by wind power and transmission system usage derived from the MP algorithm is allocated to the countries. The European power system comprises five synchronous zones of heterogeneous sizes. As displayed in Figure 3 these are the synchronous grid of Continental Europe (blue), representing the largest with 24 countries, the North of Europe (grey), the Baltic States (pink), United Kingdom (brown) and Ireland (light green). They are interconnected by HVDC lines in dark green.

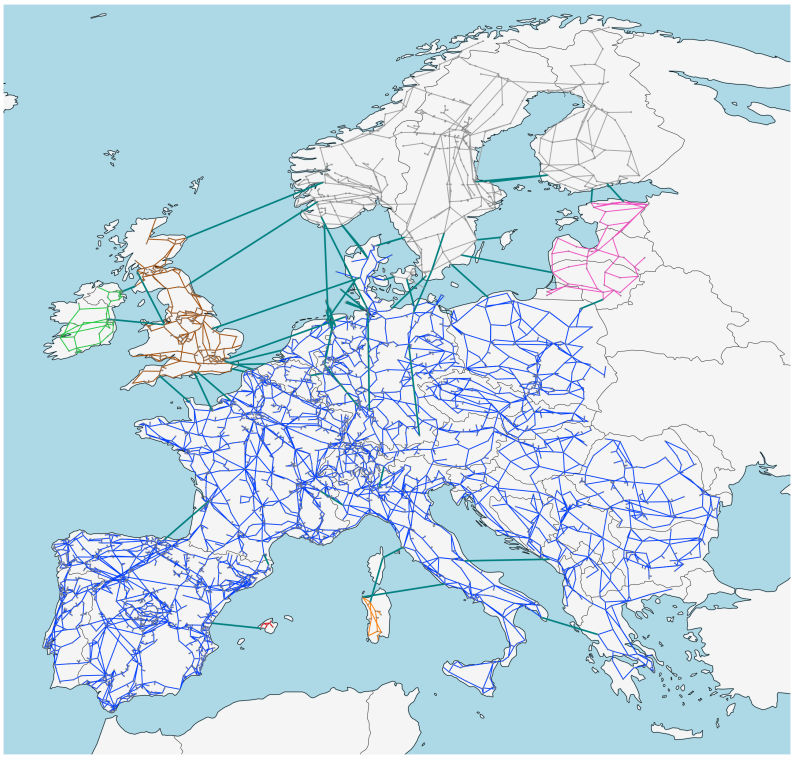

Figure 3. The different synchronous zones of the European power system, as indicated by the different colors. Whereas the Continental European grid is the largest subnetwork, Ireland, United Kingdom, Scandinavia (with only parts of Denmark) and the Baltic region have their own synchronous zone. These are interconnected via DC lines (dark green).

Each synchronous zone distributes power through AC lines and, in nominal operational state, levels out all load within the subnetwork. The power flow on the *passive* AC lines are determined by the Kirchhoff Current Law and Kirchhoff Voltage Law and are in direct relation to the nodal power injection. Therefore, when the line loading of passive branches is getting close to the capacity limits, Transmission System Operators (TSO) have to regulate and reduce the critical power flows by redispatching. However, with upcoming HVDC projects realized within the Ten Year Network Development Plan (TYNDP) [18] more controllable elements will allow to distribute power more efficiently.

The openly available power system model PyPSA-EUR, presented in [19] and available at [20], suits due to it's realistic topology representing a realistic European meshed AC-DC network. The model itself is based on refined data of the European transmission system containing all substations and AC lines at and above 220 kV, all HVDC lines as well as most of today's conventional generators. It is accessible via an automated software pipeline, which allows to examine different scenarios, *e.g.* by varying transmission network expansion limits, CO_2 caps or coupling of the heat, transport and electricity sector as done by Brown et al. [21]. In order to represent a highly-renewable future scenario, the network is clustered, simplified and linearly cost-optimized allowing generator expansion and 18% total transmission capacity expansion. Further, the CO_2 cap is set to 5% of the 1990's emission level. Available generation technologies are onshore and offshore wind, solar PV, natural gas and Run-of-River.

Available storage technologies are pumped-hydro-storage (PHS), hydro dams, batteries and hydrogen storage. Note that hydro dams (hydro) do not have the ability to store power from the

Preprints (www.preprints.org) | NOT PEER-REVIEWED | Posted: 29 January 2020 doi:10.20944/preprints202001.0352.v1

Peer-reviewed version available at Energies 2020, 13, 1233; doi:10.3390/en13051233

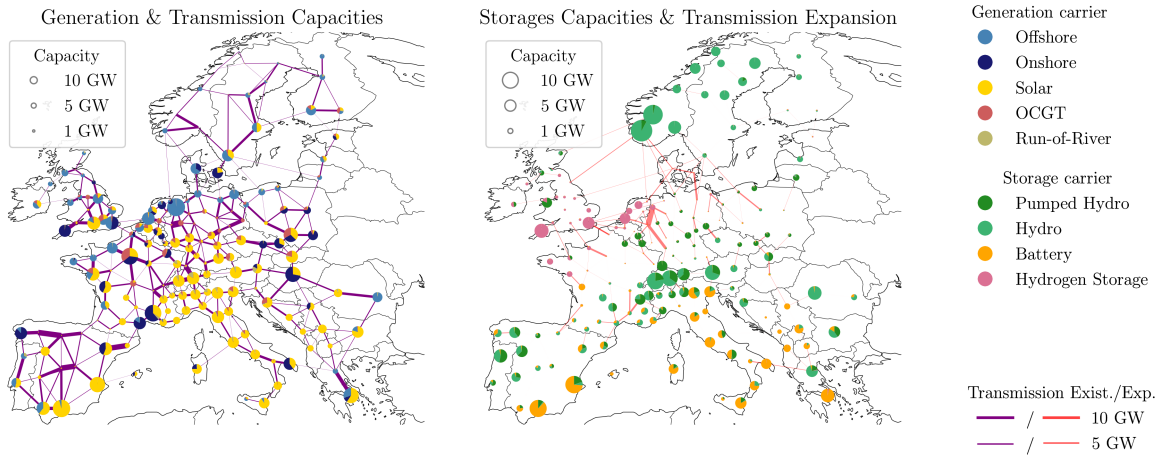

Figure 4. Highly-renewable PyPSA-EUR network with 181 nodes, 325 AC lines and 48 controllable DC links. Two scenarios are investigated, one without network expansion and one with 18% expansion relative to today's total transmission volume.

electricity grid, but are supplied by natural water inflow. All generator and storage types are allowed to be expanded except for PHS and hydro. Dispatch and expansion were calculated using the linear power flow approximation, neglecting line losses, and minimizing the total system costs consisting of capital and operational expenditures of the different network components. The resulting network, shown in Figure 4, comprises N=181 buses and L=373 lines, of which 48 are controllable DC lines. The left hand side shows power generation and original transmission capacities, the right side shows capacity distribution of storages and transmission expansion. The energy production is strongly relying on wind power, which produces 40% of the yearly total in offshore regions and 18% in onshore regions. Solar power on the other hand accounts for 23% of the total energy production. The rest is covered be hydro power (10%), Open Cycle Gas Turbines (5%) and Run-of-River (4%). The average electricity price lays at 58 €/MWh.

The two FA methods are applied on the whole simulation year, which consists of 2920 time steps representing a three hour time-resolution. We choose the standard formulation with $q = 0.5$, where the difference between MP and EBE are expected to be the largest. As the analysis of the three dimensional data $\tilde{\mathbf{P}}(t)$ and $\tilde{\mathbf{F}}(t)$ requires detailed reporting, we want to restrict on international power traffics for the following.

Figure 5(a) shows the average source-sink allocation, given by $\mathbf{A}_{\mathrm{MP}} = \mathbf{A}_{\mathrm{EBE}}$, aggregated to countries. Colors of the outer circle indicate the overall exchange of the considered country. Colors of the inner circle and inbound connections represent either exports of the country (same color as outer circle) or imports from other countries (corresponding colors of other countries in the outer circle). Self-assigned allocations are connections with the country itself, as one can clearly see for *e.g.* Germany. The allocated cross border flows (CBF) are dominated by large exporters and importers in the system. Therefore, only 12 countries with the largest cross border exchange are represented separately, whereas the remaining countries are aggregated in 'Other'. In the cost-optimized setup Germany, France and United Kingdom are the strongest exporters and importers. However, there are countries having a much higher export-import ratio, as for example Greece or Netherlands. Note that by definition of the peer-to-peer relations for both methods eq. (18) does not takes geographical distance into account thus leads to large-distance exchanges, *e.g.* Germany-Spain or Finland-Italy. However, neighboring countries disclose the strongest interconnections. On the one hand this applies particularly to countries along the North Sea coast where transmission expansion allows strong interactions. On the other hand, optimizing the cost of capacity expansion and disposition may lead to more installation and generation in regions near load centers. The FA methods now allow to further breakdown the cross border flow allocation. Figure 5(b) shows the same setup but only includes power

Preprints (www.preprints.org) | NOT PEER-REVIEWED | Posted: 29 January 2020 doi:10.20944/preprints202001.0352.v1

Peer-reviewed version available at Energies 2020, 13, 1233; doi:10.3390/en13051233

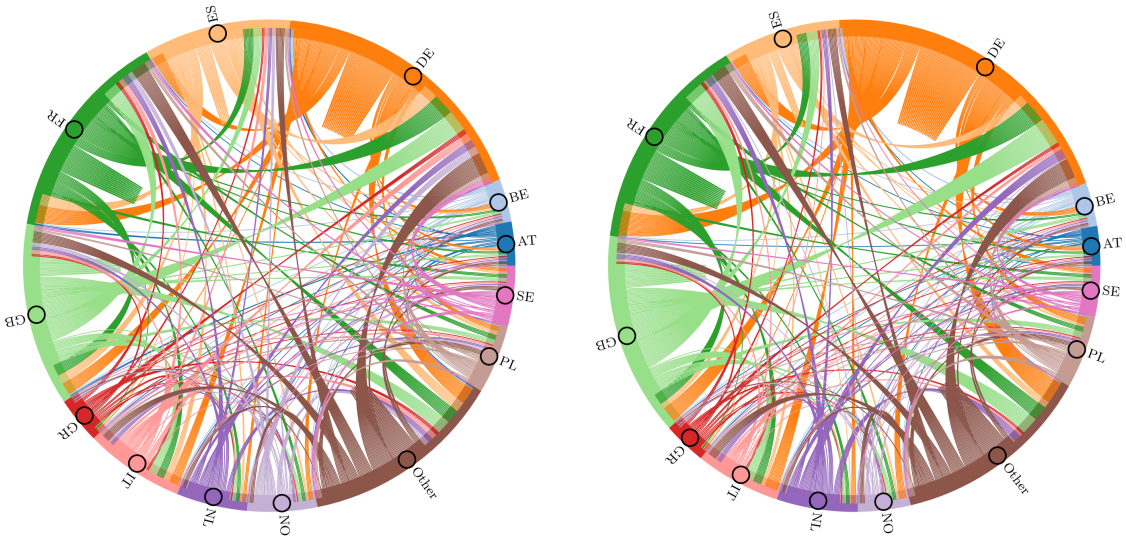

(a) Full peer-to-peer allocation

(b) Peer-to-peer allocation induced by wind power

Figure 5. Average interconnecting flow between 12 strongest exchanging countries, remaining countries are grouped into 'Other'. These aggregated source-sink relations count for both MP and EBE. On one hand the flow allocation leads to broad connections between countries which are geographically far apart, on the other hand neighboring countries reveal the strongest interconnections. Where (a) shows the full allocation, figure (b) allocates the flow induced by **wind power** only, This allocation accounts to 69% of the full cross border flow. Countries along the North Sea coast where most of the wind production is situated, dominate the allocation. Prominent differences to the total flow allocation can be found in Spain which mainly exports solar power

transfers induced by wind power injection. Remarkably, the country-to-country allocation hardly changes as the overall CBF allocation is mainly driven by countries with strong wind production. Indeed, CBF induced by wind power covers 69% of the total CBF.

As the peer-to-peer relations are dominated by strong exporters of power, we want to have a look at the transmission grid usage, which is given by $\tilde{\mathbf{F}}$. Especially, the usage of the transmission expansion might be of current interest in regard to cost allocation of grid expansion projects. Therefore, we split the flow $\underline{\mathbf{f}}$ into two categories:

- a flow on a line stays within the bounds of today's line capacities, or
- a flow exceeds the original transmission capacity, thus makes use of the 18% transmission expansion

In figs. 6(a) and 6(b) the average induced transmission for each country is shown. Each bar is split according to the two categories. First of all it is remarkable how similar EBE and MP correlate on aggregated country level. Despite strong absolute differences, the relative proportions are almost the same. The strongest transmission grid users are Great Britain, France, Germany and Spain, followed by Norway after a large gap. More or less similarly are the usages of transmission expansion distributed. So, even though Great Britain is not the strongest power exporter or importer, it has the highest average share of flows in the system. This indicates that due to its topological situation and injection behavior, its power exports and imports are, in average, of longer spatial distance, which pushes the usage of the original and expanded transmission grid.

The transmission grid usage strongly anti-correlates with the amount of storage capacity. Thus countries like Italy which have high solar power shares and strong battery storage capacities, have proportionally dependence on the transmission grid. Thus, for a simplified approach of allocating

Preprints (www.preprints.org) | NOT PEER-REVIEWED | Posted: 29 January 2020 doi:10.20944/preprints202001.0352.v1

Peer-reviewed version available at Energies 2020, 13, 1233; doi:10.3390/en13051233

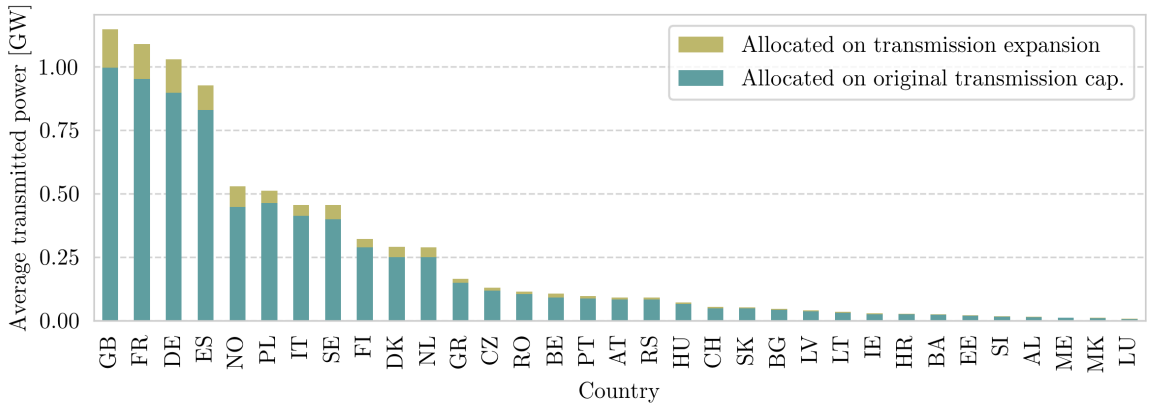

(a) Equivalent Bilateral Exchanges

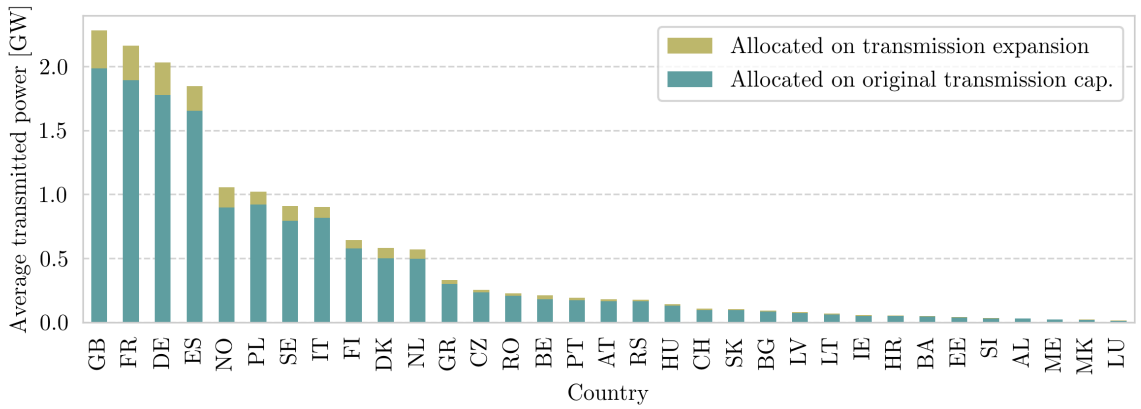

(b) Marginal Participation

Figure 6. Country-wise flow allocation using Equivalent Bilateral Exchanges (a) and Marginal Participation (b). The flow allocation per country is split into two parts, one for flows which make use of transmission expansion and one for flows which stay within the original capacity bounds. Both methods (fig. 6(a)) state that Great Britain is the strongest user of the transmission grid who however is not the strongest trader of power in the renewable network simulation, as found Figure 5.

capital and operational expenditures of the transmission grid to countries, one can legitimately propose to allocate capital expenditures proportional to the use of transmission expansion flow (the upper parts of the bars) and operational expenditures proportional to the flow allocation within the original capacity bound (lower parts).

Finally, we close with a short discussion about higher absolute flow contributions in the MP allocation compared to EBE. As pointed out earlier, with the 50%-50% split the MP algorithm leads to effective flows from net producer to net producer. This leads to a higher shares of counter flows in the allocation, which on the other hand have to be balanced according to eq. (7). Figure 7 shows the ratio between the sum of absolute allocated flows and the total transmission as a function of q. Indeed, in the realm $0 < q < 1$ the MP method allocates much more flow, peaking at $q = 0.5$ with more than 6 times of the total transmitted power, whereas the EBE method stays steadily at around 3 times of the total transmission. The two lower lines reflect the sum of all allocated counter-flows which, as to expect, lays 0.5 below the half of the absolute allocation sums. In other words, each counter-flow cancels out with an aligned flow, and the remaining aligned flows sum up to $\underline{\mathbf{f}}$.

Note that it can be assumed that this effect scales with the network resolution, as the number of possible peer-to-peer connections scales with $\mathcal{O}\left(N^2\right)$. For $q = 0.5$, $\tilde{\mathbf{P}}_{\text{mp}}$ exploits all of these connections,

Preprints (www.preprints.org) | NOT PEER-REVIEWED | Posted: 29 January 2020 doi:10.20944/preprints202001.0352.v1

Peer-reviewed version available at Energies 2020, 13, 1233; doi:10.3390/en13051233

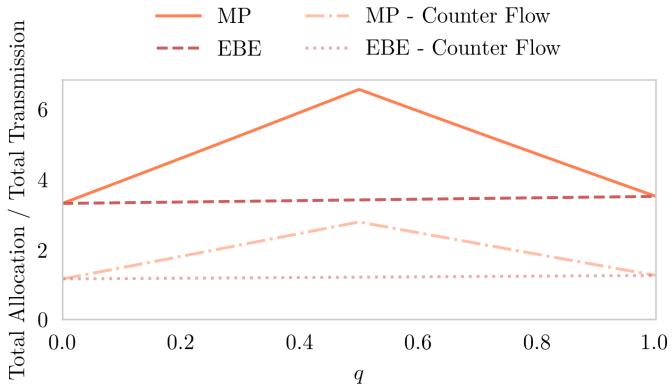

Figure 7. Total allocated flow of an exemplary snapshot in the network for both allocation methods, Marginal Participation (MP) and Equivalent Bilateral Exchanges (EBE) as a function of the shift parameter q. Whereas $q = 0$ and $q = 1$ result in the same allocation, the MP algorithm allocates more counter-flows the more q approximates $q = 0.5$ (the standard MP setup), which is due to a strong increase of counter flows.

which makes the appearance of counter-flows much more likely. However further research needs to be done to sustain this argument.

5. Summary and Conclusions

A mathematical consistent extension of the Power Transfer Distribution Factors matrix (PTDF) which incorporates the operational state of controllable elements as high-voltage direct current lines was presented. By introducing a flow dependent pseudo-impedance vector $\bar{\omega}(\underline{\mathbf{f}})$ of the size of controllable elements in the grid, the PTDF matrix was reformulated for meshed AC-DC networks. Thereby, it becomes essential to differentiate between the controllable elements being part of a independent cycle in the network or not, as both cases are affected by a different set of physical constraints. The extension was propagated to the reformulated and extended Marginal Participation and Equivalent Bilateral Exchanges algorithm, flow allocation methods which are both based on the PTDF matrix. Thereby, both algorithms become applicable for meshed AC-DC networks and thus for the European power system. On the basis of a future scenario model of the European power system a flow allocation was performed to determine cross border transactions and transmission grid usage per country. It could be shown that the FA methods can appropriately be used to quantify the usage of transmission expansion and opens a possible distribution scheme for capital expenditures on transmission projects.

Author Contributions: Conceptualization, F.H. and M.S.; methodology, F.H.; software, F.H.; validation, F.H., M.S. and A.K.; formal analysis, F.H.; investigation, F.H.; resources, F.H.; data curation, F.H.; writing–original draft preparation, F.H.; writing–review and editing, F.H, M.S, A.K.; visualization, F.H.; supervision, H.S.; project administration, H.S.; funding acquisition, A.K., H.S. All authors have read and agreed to the published version of the manuscript.

Funding: This research was funded by the by the German Federal Ministry for Economics Affairs and Energy in the frame of the NetAllok project [22].

Acknowledgments: We thank Mirko Schäfer and Tom Brown for stready support and fruitful discussions.

Conflicts of Interest: The authors declare no conflict of interest.

1. Jiuping Pan.; Teklu, Y.; Rahman, S.; Jun, K. Review of Usage-Based Transmission Cost Allocation Methods under Open Access. *IEEE Transactions on Power Systems* **Nov./2000**, *15*, 1218–1224. doi:10.1109/59.898093.

Preprints (www.preprints.org) | NOT PEER-REVIEWED | Posted: 29 January 2020 doi:10.20944/preprints202001.0352.v1

Peer-reviewed version available at Energies 2020, 13, 1233; doi:10.3390/en13051233

2. Bialek, J. Tracing the Flow of Electricity. *IEE Proceedings - Generation, Transmission and Distribution* **1996**, *143*, 313. doi:10.1049/ip-gtd:19960461.
3. Hörsch, J.; Schäfer, M.; Becker, S.; Schramm, S.; Greiner, M. Flow Tracing as a Tool Set for the Analysis of Networked Large-Scale Renewable Electricity Systems. *International Journal of Electrical Power & Energy Systems* **2018**, *96*, 390–397. doi:10.1016/j.ijepes.2017.10.024.
4. Conejo, A.J.; Contreras, J.; Lima, D.A.; Padilha-Feltrin, A. Z-Bus Transmission Network Cost Allocation. *IEEE Transactions on Power Systems* **2007**, *22*, 342–349. doi:10.1109/TPWRS.2006.889138.
5. Chen, Y.C.; Dhople, S.V. Power Divider. *IEEE Transactions on Power Systems* **2016**, *31*, 5135–5143. doi:10.1109/TPWRS.2016.2519900.
6. Chang, Y.C.; Lu, C.N. An Electricity Tracing Method with Application to Power Loss Allocation. *International Journal of Electrical Power & Energy Systems* **2001**, *23*, 13–17. doi:10.1016/S0142-0615(00)00037-5.
7. Rudnick, H.; Palma, R.; Fernandez, J. Marginal Pricing and Supplement Cost Allocation in Transmission Open Access. *IEEE Transactions on Power Systems* **1995**, *10*, 1125–1132. doi:10.1109/59.387960.
8. Galiana, F.; Conejo, A.; Gil, H. Transmission Network Cost Allocation Based on Equivalent Bilateral Exchanges. *IEEE Transactions on Power Systems* **2003**, *18*, 1425–1431. doi:10.1109/TPWRS.2003.818689.
9. Hadush, S.Y.; De Jonghe, C.; Belmans, R. The Implication of the European Inter-TSO Compensation Mechanism for Cross-Border Electricity Transmission Investments. *International Journal of Electrical Power & Energy Systems* **2015**, *73*, 674–683. doi:10.1016/j.ijepes.2015.05.041.
10. Banez-Chicharro, F.; Olmos, L.; Ramos, A.; Latorre, J.M. Beneficiaries of Transmission Expansion Projects of an Expansion Plan: An Aumann-Shapley Approach. *Applied Energy* **2017**, *195*, 382–401. doi:10.1016/j.apenergy.2017.03.061.
11. Baroche, T.; Pinson, P.; Latimier., R.L.G.; Ahmed, H.B. Exogenous Approach to Grid Cost Allocation in Peer-to-Peer Electricity Markets. *arXiv:1803.02159 [cs, math]* **2018**, [arXiv:cs, math/1803.02159].
12. Schäfer, M.; Tranberg, B.; Hempel, S.; Schramm, S.; Greiner, M. Decompositions of Injection Patterns for Nodal Flow Allocation in Renewable Electricity Networks. *The European Physical Journal B* **2017**, *90*, 144. doi:10.1140/epjb/e2017-80200-y.
13. Tranberg, B.; Corradi, O.; Lajoie, B.; Gibon, T.; Staffell, I.; Andresen, G.B. Real-Time Carbon Accounting Method for the European Electricity Markets. *Energy Strategy Reviews* **2019**, *26*, 100367. doi:10.1016/j.esr.2019.100367.
14. Brown, T. Transmission Network Loading in Europe with High Shares of Renewables. *IET Renewable Power Generation* **2015**, *9*, 57–65. doi:10.1049/iet-rpg.2014.0114.
15. Ronellenfitsch, H.; Timme, M.; Witthaut, D. A Dual Method for Computing Power Transfer Distribution Factors. *IEEE Transactions on Power Systems* **2016**, pp. 1–1. doi:10.1109/TPWRS.2016.2589464.
16. Ronellenfitsch, H.; Manik, D.; Horsch, J.; Brown, T.; Witthaut, D. Dual Theory of Transmission Line Outages. *IEEE Transactions on Power Systems* **2017**, *32*, 4060–4068. doi:10.1109/TPWRS.2017.2658022.
17. Gil, H.; Galiana, F.; Conejo, A. Multiarea Transmission Network Cost Allocation. *IEEE Transactions on Power Systems* **2005**, *20*, 1293–1301. doi:10.1109/TPWRS.2005.851951.
18. ENTSO-E. TYNDP2016, Projects. Technical report.
19. Hörsch, J.; Hofmann, F.; Schlachtberger, D.; Brown, T. PyPSA-Eur: An Open Optimisation Model of the European Transmission System. *Energy Strategy Reviews* **2018**, *22*, 207–215. doi:10.1016/j.esr.2018.08.012.
20. Hörsch, J.; Neumann, F.; Hofmann, F.; Schlachtberger, D.; Brown, T. PyPSA-Eur: An Open Optimisation Model of the European Transmission System (Code), 2020.
21. Brown, T.; Schlachtberger, D.; Kies, A.; Schramm, S.; Greiner, M. Synergies of Sector Coupling and Transmission Reinforcement in a Cost-Optimised, Highly Renewable European Energy System. *Energy* **2018**, *160*, 720–739. doi:10.1016/j.energy.2018.06.222.
22. Bundesministerium für Wirtschaft und Energie. Verbundvorhaben: NET-ALLOK - Methoden Und Anwendungen Der Netzkostenallokation, Teilvorhaben: Methoden Und Analyse von Kostenallokationsmethoden Im Betrieb Des Elektrizitätssystems. https://www.enargus.de/pub/bscw.cgi/?op=enargus.eps2&v=10&s=14&q=EA3310&id=399670&p=10.